Molecular three-continuum approximation for ionization of H_2 by electron impact

C. R. Stia,[1] O. A. Fojón,[1,2] P. F. Weck,[1,3] J. Hanssen,[3] B. Joulakian,[3] and R. D. Rivarola[1,2]
[1]*Instituto de Física Rosario, CONICET-UNR, Avenida Pellegrini 250, 2000 Rosario, Argentina*
[2]*Escuela de Ciencias Exactas y Naturales, Facultad de Ciencias Exactas, Ingeniería y Agrimensura, Universidad Nacional de Rosario, 2000 Rosario, Argentina*
[3]*Institut de Physique, Laboratoire de Physique Moléculaire et des Collisions, Université de Metz, Technopôle 2000, 1 Boulevard Arago, 57078 Metz Cedex 3, France*
(Received 3 June 2002; published 14 November 2002)

A molecular three-continuum-type approximation is developed to study the $(e,2e)$ reaction for H_2 targets. The molecular nature of the target is treated within the framework of a two-effective-center approximation. The correlate motion of the particles in the final channel of the reaction is taken into account by an adequate product of Coulomb functions. Triple differential cross sections are computed. A good agreement with the available experiments is obtained.

DOI: 10.1103/PhysRevA.66.052709 PACS number(s): 34.80.Gs

I. INTRODUCTION

Interaction of electrons with atoms and molecules is of interest in many fields such as astrophysics, plasma production (including plasma-etching mechanisms of great importance, for instance, in the design of semiconductor devices), planetary and upper-atmosphere reactions and irradiation of living matter [1]. All mentioned areas need a full understanding of the mechanisms involved in electron-atom and -molecule collisions. This is not surprising if one realizes that structure, properties, and processes of matter depend ultimately upon interactions between electrons, atoms, and molecules.

Ionization of atoms by electron impact has been widely studied, both theoretically and experimentally. In the case of single ionization, this reaction leads to three unbound charged particles interacting through Coulomb potentials in the final channel. An exact quantum solution for this three-body problem is not known yet. Several theoretical approximations were developed to describe the dynamics of ionization by electron-impact ranging from the first order of a Born series (FBA) in which the incident and the scattered electrons are represented by plane waves to much more elaborated approaches. Of particular interest in this work is the approximation given by Brauner, Briggs, and Klar (hereafter BBK) [2] to study ionization of H atoms. It is worthy to mention that a version of this approximation was previously developed for impact of ions [3]. In the BBK approach, the exact final-state wave function is obtained in an approximate way as a product of three Coulomb functions. Consequently, the correlate motion of the particles interacting through long-range potentials in the final state is properly taken into account. BBK predictions were in agreement with the available experimental results of triple differential cross sections (TDCS) for atomic H [4] in coplanar asymmetric geometry (in this arrangement, the incident, the scattered, and the ejected electrons belong to the same plane; and the scattered and ejected electron energies differ considerably). TDCS bring detailed information about the dynamics of the reaction constituting one of the most stringent tests to theories.

The study of ionization of molecular species has advanced in a slower way than the atomic ones. On the experimental side, it has not been possible yet to prepare the molecular target in a particular rovibrational state. Another great problem to be solved is the finite resolution of the electron beam. In general, the rotational and the vibrational states of the molecules cannot be resolved during a collision experiment. On the theoretical side, these extra degrees of freedom complicate the theoretical description of the reaction. In addition, the molecular structure must be fully included in any realistic description of the process. This requires the representation of the continuum states of the scattered and emitted electrons in the field of the residual molecular target. Even for the simplest diatomic molecules, such as H_2, an exact treatment of the involved wave functions renders the collisional problem almost untractable. Therefore, several approximations have been developed.

H_2 targets have received a lot of attention as they may serve as a test case containing most of the complications of molecular targets. Indeed, it has been a matter of active research over the past 25 years [5–9]. There exist TDCS measurements for this target, a set of TDCS obtained in a relative scale [5] and another one of absolute TDCS obtained at much higher impact energies [8]. On the theoretical front, different perturbative models were developed. For highly asymmetric coplanar geometries, FBA was used. The ionized electron was described in previous works by a plane-wave [10,11] or by a continuum wave function corresponding to a *one-center* Coulomb potential of *effective* charge $Z_{eff}=1$ placed at the center of mass of the molecule [12]. More elaborated continuum wave functions were also developed by using a *one-center* potential including the interaction between the ionized electron and the residual target (assuming that the ionic core remains frozen during the reaction) [12]. Two-center partial-wave [13] and two-center continuum [14] calculations were also performed for H_2.

Recently, a *two-effective-center* approximation (TEC) was introduced [15]. In this model, it is assumed that ionization of the *active* electron takes place more likely in the neigh-

borhoods of each molecular nuclei. The *passive* electron is supposed to screen completely the nucleus from which ionization is not produced. Thus, the continuum wave function of the ejected electron is proposed as a simple product of a plane wave centered at the molecule mass center and *one-center* continuum factors of charge $Z_T=1$. These *one-center* continuum factors describe the interaction of the ionized electron with each molecular center. One of the advantages of the TEC approximation is that the numerical evaluation of transition matrix elements is greatly simplified. The TEC model is expected to work well at sufficiently high impact energies. As a matter of fact, TDCS obtained with the TEC approximation were in good agreement with absolute measurements [8] in this energy regime. As the impact energy decreases, the inclusion of all mutual interactions present in the final channel and not taken into account in the TEC approximation is crucial. A good candidate to extend the domain of validity of the TEC approximation to lower impact energies is the BBK approximation. In spite of its success in the atomic domain, it is not surprising that so far no extension of this model has been attempted to the case of molecular targets. It is not easy to handle all the continuum functions that such an extension require. In a recent work, atomic BBK TDCS for electron and positron impact on H_2 were computed [16] to compare with a kinematically complete experiment in which hydrogen molecules are ionized using positron as projectiles [17]. In these BBK calculations, the H_2 target is assumed to be composed of two noninteracting hydrogen atoms with binding energy equal to the ionization energy of the H molecule.

In the present work, a molecular BBK-type (MBBK) approximation is developed within the framework of the TEC approximation. In the formulation, virtues of both BBK and TEC are exploited. On one hand, the TEC model is used to take into account in a simple but efficient way the molecular nature of the target as well as the influence of the passive electron on the reaction. On the other hand, the BBK approximation is used to include in a proper way the correlate motion of the unbound charged particles in the final channel of the reaction.

Atomic units will be used except where otherwise stated.

II. THEORY

The reaction of interest is the electron-impact ionization of H_2 molecular targets, namely,

$$e^- + \mathrm{H}_2(^1\Sigma_g^+) \rightarrow 2e^- + \mathrm{H}_2^+(^2\Sigma_g^+). \tag{1}$$

The incident direction defined by the wave vector $\mathbf{k}_i$ of the incident electron is taken as the *z*-quantization axis.

As experiments were performed so far only with low-energy resolution, closure relations can be applied over all possible final rotational and vibrational states of the residual target and the ionization process may be considered as a pure electronic transition [11,12]. Moreover, molecules are not oriented in the experiments. So, an average over all possible orientations of the molecular axis with an uniform probability distribution must be done in obtaining observable quantities. At the energies considered in this work, the collision time is much smaller than the vibrational and rotational periods involved. Consequently, the molecule can be considered as frozen thoughout all the reaction. In particular, the internuclear distance remains unchanged. Therefore, only vertical transitions from the ground electronic state of the target to the ground electronic state of the residual H_2^+ are considered in this work. Moreover, as only highly asymmetric arrangements are studied, exchange effects in the collision dynamics may be disregarded.

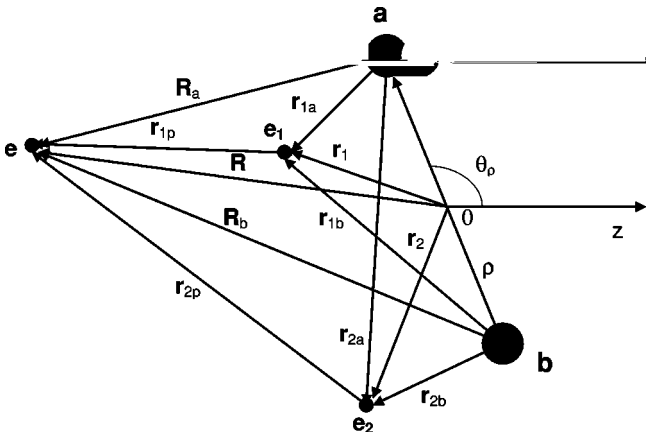

FIG. 1. Coordinates used in the text.

The triple differential cross section is given by the following expression [15]:

$$\sigma^{(3)} = \frac{d^3\sigma}{d\Omega_e d\Omega_s d(k_e^2/2)} \cong 2\frac{1}{4\pi}(2\pi)^4 \frac{k_e k_s}{k_i} \int d\Omega_\rho |t_{fi}^e(\boldsymbol{\rho}_0)|^2, \tag{2}$$

where the emitted electron is ejected with momentum $\mathbf{k}_e$ into the differential solid angle Ω_e with respect to the incidence direction, and the projectile is scattered with momentum $\mathbf{k}_s$ into the solid angle Ω_s. In Eq. (2), $\boldsymbol{\rho}_0$ denotes the equilibrium internuclear vector of the molecular target.

The *prior* version of the transition matrix element reads

$$t_{fi}^e(\boldsymbol{\rho}_0) = \langle \Psi_f^-(\boldsymbol{\rho}_0, \mathbf{R}, \mathbf{r}_1, \mathbf{r}_2) | V_i | \Psi_i^+(\boldsymbol{\rho}_0, \mathbf{R}, \mathbf{r}_1, \mathbf{r}_2) \rangle, \tag{3}$$

where Ψ_i^+ is the nonperturbed electronic wave function in the initial channel and Ψ_f^- is the final exact electronic wave function with correct asymptotic conditions. Coordinates are described in the laboratory system and are sketched in Fig. 1. V_i is the perturbation in the entrance channel, given by

$$V_i = \frac{1}{r_{1p}} + \frac{1}{r_{2p}} - \frac{Z_T}{R_a} - \frac{Z_T}{R_b}, \tag{4}$$

with $Z_T=1$, being the charge of the molecular nuclei.

The initial nonperturbed wave function Ψ_i^+ is represented as

$$\Psi_i^+ = \frac{e^{i\mathbf{k}_i \cdot \mathbf{R}}}{(2\pi)^{3/2}} \Phi_i(\rho, \mathbf{r}_1, \mathbf{r}_2), \tag{5}$$

where Φ_i is the initial molecular bound state that (in this work) is described by the Heitler-London-type wave function proposed by Wang [18],

$$\Phi_i(\rho_0,\mathbf{r}_1,\mathbf{r}_2)=N_{HL}(\rho_0)\{e^{-\alpha^* r_{1a}}e^{-\alpha^* r_{2b}} + e^{-\alpha^* r_{1b}}e^{-\alpha^* r_{2a}}\}, \tag{6}$$

with $\alpha^*=1.166$, $\rho_0=1.406$, and the normalization function N_{HL}.

The choice of an approximate final electronic wave function Ψ_f^- is made in the present approach within the framework of the previously developed TEC approximation for diatomic molecules [15]. In this approximation, the molecular structure is preserved. The final state of the reaction is treated as a three-body problem, namely, the scattered electron, the ejected electron, and the residual target; the latter being considered as a whole body. Ionization is assumed to be produced in the neighborhood of each molecular center. Then, if one electron is ionized from the proximities of nucleus $a(b)$, the remaining electron is assumed to screen completely the nucleus $b(a)$. In this way, the influence of the passive electron on the reaction is taken into account in an approximate way. These are the basic assumptions of the TEC model. To proceed further, a choice for the electronic final wave function has to be made. For the sake of simplicity, the choice in Ref. [15] was made within the first Born approximation, resulting in the following electronic final wave function:

$$\Psi_f^- \cong \frac{e^{i\mathbf{k}_s\cdot\mathbf{R}}}{(2\pi)^{3/2}}\Phi_f(\rho,\mathbf{r}_2)\xi_c, \tag{7}$$

Φ_f is the wave function corresponding to the bound state of the residual H_2^+ molecular ion represented in the present work by a simple linear combination of atomic orbitals,

$$\Phi_f(\rho,\mathbf{r}_2)=N_f(\rho)\{e^{-\alpha r_{2a}}+e^{-\alpha r_{2b}}\}, \tag{8}$$

with $N_f(\rho)$ being the normalization factor and $\alpha=1.3918$ being the variational parameter. As it is supposed that transitions are produced at fixed distances $\rho_0=1.406$ (*vertical* transitions), $N_f(\rho_0)$ is used in the calculations.

The function ξ_c in Eq. (7) was chosen in Ref. [15] as

$$\xi_c=\xi_c(\mathbf{k}_e,\mathbf{r}_1)=\frac{e^{i\mathbf{k}_e\cdot\mathbf{r}_1}}{(2\pi)^{3/2}}C(\mathbf{k}_e,\mathbf{r}_{1j},-Z_T/k_e), \tag{9}$$

where $j=a$ or b. The function ξ_c corresponding to $j=a(b)$ is used when the exponential term $e^{-\alpha^* r_{1a}}(e^{-\alpha^* r_{1b}})$ is present in the matrix transition element given by Eq. (3). This is in agreement with one of the basic assumptions of the TEC approximation, namely, when the active electron is ionized from the proximities of one molecular center, the passive electron completely screens the other one. The Coulomb factor $C(\mathbf{k},\mathbf{r},\gamma)$ in Eq. (9) reads

$$C(\mathbf{k},\mathbf{r},\gamma)=\Gamma(1-i\gamma)e^{-\pi\gamma/2}\,{}_1F_1(i\gamma;1;-i(kr+\mathbf{k}\cdot\mathbf{r})). \tag{10}$$

In Eq. (7), it is supposed that electron 1 is ionized. The exchange with electron 2 is taken into account by means of the factor 2 in Eq. (2).

This simple first-order version of the TEC model makes the computation of the transition matrix elements simple. Moreover, at the energies considered in Ref. [15], a first-order approximation may be considered as appropriate to describe the collision process. However, as the impact energy decreases, the correlate motion of the three particles in the final channel must be included. The TEC model is particularly suitable to perform this operation. Instead of the simple one-center Coulomb function employed in Eq. (9), a more elaborate correlated one may be used. In this work, the choice is made in a similar way to the BBK approximation for atoms, leading to the following function:

$$\xi_c=\xi_c(\mathbf{k}_e,\mathbf{k}_s,\mathbf{R},\{\mathbf{r}\}) = \frac{e^{i\mathbf{k}_e\cdot\mathbf{r}_1}}{(2\pi)^{3/2}}C(\mathbf{k}_e,\mathbf{r}_{1j},\gamma_e)C(\mathbf{k}_s,\mathbf{R}_j,\gamma_s)C(\mathbf{k}_{1p},\mathbf{r}_{1p},\gamma_{ep}), \tag{11}$$

where $\{\mathbf{r}\}$ represents the ensemble of the target electron coordinates, and the Sommerfeld parameters γ_e,γ_s, and γ_{ep} are given by

$$\gamma_s=-Z_T/k_s,\qquad \gamma_e=-Z_T/k_e,\qquad \gamma_{ep}=\frac{1}{2k_{1p}}. \tag{12}$$

Here, $\mathbf{k}_{1p}=\frac{1}{2}(\mathbf{k}_s-\mathbf{k}_e)$ is the momentum conjugate to $\mathbf{r}_{1p}$.

The function ξ_c describes the mutual interactions between the three bodies in the final channel of the reaction through the use of Coulomb functions. Again, the basic assumptions of the TEC model are exploited to achieve this end.

So, the transition matrix element [Eq. (3)] for the MBBK approximation reads

$$t_{fi}^e(\boldsymbol{\rho})\simeq\frac{1}{(2\pi)^{9/2}}NN_f(\rho_0)N_{HL}(\rho_0)\Big\langle e^{i\mathbf{k}_e\cdot\mathbf{r}_1} \times{}_1F_1(i\gamma_e;1;-i(k_e r_{1j}+\mathbf{k}_e\cdot\mathbf{r}_{1j})) \times{}_1F_1(i\gamma_s;1;-i(k_s R_j+\mathbf{k}_s\cdot\mathbf{R}_j))\,{}_1F_1(i\gamma_{ep};1; -i(k_{1p}r_{1p}+\mathbf{k}_{1p}\cdot\mathbf{r}_{1p}))\;(e^{-\alpha r_{2a}}+e^{-\alpha r_{2b}}) \times\left|\left(\frac{1}{r_{1p}}+\frac{1}{r_{2p}}-\frac{1}{R_a}-\frac{1}{R_b}\right)\right| \times e^{i\mathbf{K}\cdot\mathbf{R}}(e^{-\alpha^* r_{1a}}\;\;e^{-\alpha^* r_{2b}}+e^{-\alpha^* r_{1b}}\;\;e^{-\alpha^* r_{2a}})\Big\rangle, \tag{13}$$

with $j=a$ or b, the momentum transfer $\mathbf{K}=\mathbf{k}_i-\mathbf{k}_s$, and

$$N=\Gamma(1+i\gamma_e)\Gamma(1+i\gamma_s)\times\Gamma(1+i\gamma_{ep})\exp[-\pi(\gamma_e+\gamma_s+\gamma_{ep})/2]. \quad (14)$$

In the computation of TDCS, one additional approximation is made. The matrix element may be written as a sum of direct and indirect terms as follows:

$$t_{fi}^{e}(\boldsymbol{\rho}_0)=\sum_{\substack{j,l\\ j\neq l}}(t_{j,l}^{dir}+t_{j,l}^{ind}),\quad j,l=a,b, \quad (15)$$

where

$$t_{j,l}^{dir}\propto\left\langle e^{i\mathbf{k}_e\cdot\mathbf{r}_1}\,{}_1F_1(i\gamma_e;1;-i(k_e r_{1j}+\mathbf{k}_e\cdot\mathbf{r}_{1j}))\times{}_1F_1(i\gamma_s;1;-i(k_s R_j+\mathbf{k}_s\cdot\mathbf{R}_j))\,{}_1F_1(i\gamma_{ep};1;-i(k_{1p}r_{1p}+\mathbf{k}_{1p}\cdot\mathbf{r}_{1p}))\;(e^{-\alpha r_{2j}}+e^{-\alpha r_{2l}})\times\left|\left(\frac{1}{r_{1p}}-\frac{1}{R_j}\right)\right|e^{i\mathbf{K}\cdot\mathbf{R}}e^{-\alpha^* r_{1j}}e^{-\alpha^* r_{2l}}\right\rangle \quad (16)$$

and

$$t_{j,l}^{ind}\propto\left\langle e^{i\mathbf{k}_e\cdot\mathbf{r}_1}\,{}_1F_1(i\gamma_e;1;-i(k_e r_{1j}+\mathbf{k}_e\cdot\mathbf{r}_{1j}))\times{}_1F_1(i\gamma_s;1;-i(k_s R_j+\mathbf{k}_s\cdot\mathbf{R}_j))\,{}_1F_1(i\gamma_{ep};1;-i(k_{1p}r_{1p}+\mathbf{k}_{1p}\cdot\mathbf{r}_{1p}))\;(e^{-\alpha r_{2j}}+e^{-\alpha r_{2l}})\times\left|\left(\frac{1}{r_{2p}}-\frac{1}{R_l}\right)\right|e^{i\mathbf{K}\cdot\mathbf{R}}e^{-\alpha^* r_{1j}}e^{-\alpha^* r_{2l}}\right\rangle. \quad (17)$$

The direct and indirect terms may be interpreted in the following way [19]. The direct term describes ionization of electron 1 from center $j=a$ (or b) by means of the interaction of the projectile with this electron and with center j. The indirect term may be considered as giving ionization of electron 1 from center j through the interaction of the projectile with electron 2 and with the other center labeled l. Of course, electrons are shared by both nuclei in the molecule, but matrix elements admit this interpretation. The contribution of indirect terms to the TDCS has been analyzed within the first-order TEC approximation, i.e., with the function given by Eq. (9). It has been found that at the impact energies considered here, TDCS are practically not modified by neglecting the indirect terms. This supports to some extent the neglecting of them in the present approach.

The transition matrix element for the molecular BBK approximation [Eq. (13)] may be written in the following compact form:

$$t_{fi}^{e}(\boldsymbol{\rho}_0)\simeq\frac{2}{(2\pi)^{9/2}}NN_f(\rho_0)N_{HL}(\rho_0)[L(\alpha,\alpha^*)+L(\alpha+\alpha^*,0)]U(\alpha,\alpha^*;\mathbf{K},\mathbf{k}_e)\times\cos[(\mathbf{k_e}-\mathbf{K})\cdot\boldsymbol{\rho}_0/2], \quad (18)$$

where L is a two-center integral given by [20]

$$L(p,q)=\int d\mathbf{r}_2 e^{-pr_{2a}}e^{-qr_{2b}}=\frac{8\pi}{C^3\rho}[p(\rho C-4q)e^{-q\rho}+q(\rho C+4p)e^{-q\rho}], \quad (19)$$

with $C=p^2-q^2$.

U in Eq. (18) is given by

$$U(\alpha,\alpha^*;\mathbf{K},\mathbf{k}_e)=\int d\mathbf{R}_a d\mathbf{r}_{1a}e^{i\mathbf{K}\cdot\mathbf{R}_a}e^{-i\mathbf{k}_e\cdot\mathbf{r}_{1a}}e^{-\alpha^* r_{1a}}\times\left(\frac{1}{r_{1p}}-\frac{1}{R_a}\right)\times{}_1F_1(-i\gamma_e;1;i(k_e r_{1a}+\mathbf{k}_e\cdot\mathbf{r}_{1a}))\times{}_1F_1(-i\gamma_s;1;i(k_s R_a+\mathbf{k}_s\cdot\mathbf{R}_a))\times{}_1F_1(-i\gamma_{ep};1;i(k_{1p}r_{1p}+\mathbf{k}_{1p}\cdot\mathbf{r}_{1p})). \quad (20)$$

This six-dimensional integral is reduced to a three-dimensional one and then solved by numerical quadratures as in previous works [21,22].

Finally, performing the integration over all possible molecular orientations, the triple differential cross section given by Eq. (2) may be rewritten as

$$\sigma^{(3)}=\frac{d^3\sigma}{d\Omega_e d\Omega_s d(k_e^2/2)}\cong 4(2\pi)^{-5}\frac{k_e k_s}{k_i}|NN_f(\rho_0)N_{HL}(\rho_0)\times[L(\alpha,\alpha^*)+L(\alpha+\alpha^*,0)]|^2|U(\alpha,\alpha^*;\mathbf{K},\mathbf{k}_e)|^2\times\left(1+\frac{\sin(\chi\rho_0)}{\chi\rho_0}\right), \quad (21)$$

with $\boldsymbol{\chi}=\mathbf{k}_e-\mathbf{K}$.

III. RESULTS AND DISCUSSIONS

In this section, the spectra of ejected electrons in e^--H_2 ionizing collisions are analyzed. In all cases, the studied arrangements correspond to coplanar asymmetric collisions.

In Figs. 2(a)–2(c), MBBK triple differential cross sections as a function of the ejection angle θ_e and for impact and emission energies $E_i=4087$ eV and $E_e=20$ eV, respectively, are presented. Three different geometries corresponding to scattering angles $\theta_s=1°, 1.5°$, and $3°$, respectively, are shown. Experimental results from Ref. [8] are also displayed in the figures. The agreement of MBBK TDCS with experiments is very good. Only in the region of the binary peak, MBBK values seems to underestimate the measurements by a very small amount. However, the theoretical predictions are always within the experimental uncertainties. Moreover, the dispersion of experimental data is particularly marked in this angular region, specially in Figs. 2(b) and 2(c). The po-

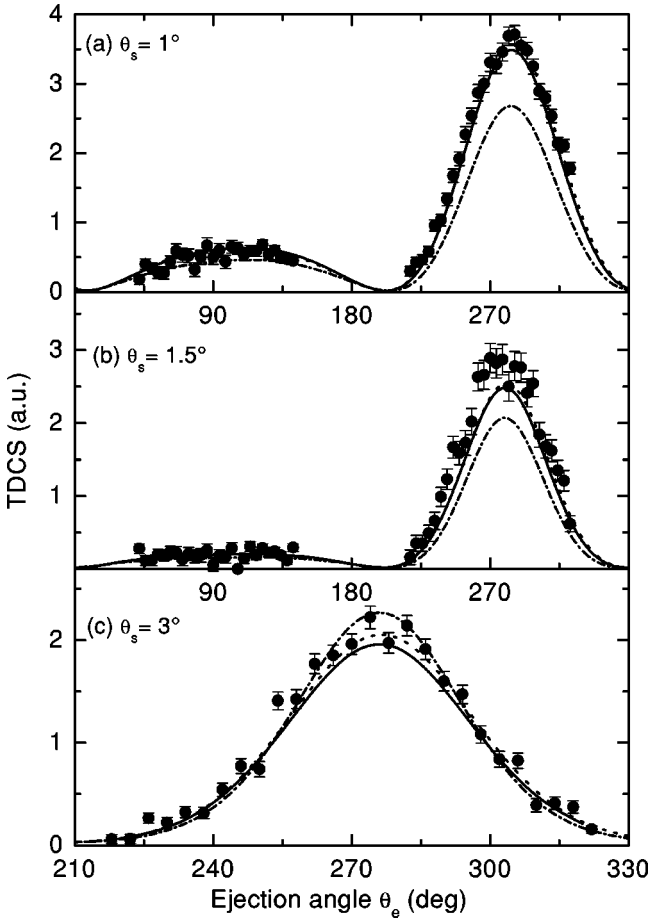

FIG. 2. Triple-differential cross sections as a function of the ejection angle θ_e. Impact energy $E_i=4087$ eV; emission energy $E_e=20$ eV; and scattering angles (a) $\theta_s=1°$, (b) $\theta_s=1.5°$, and (c) $\theta_s=3°$. Present MBBK results are represented by full line, TEC results by dotted lines, twice BBK results for effective atomic hydrogen by dashed and dotted lines, and experiments (from Ref. [8]), are represented by full circles.

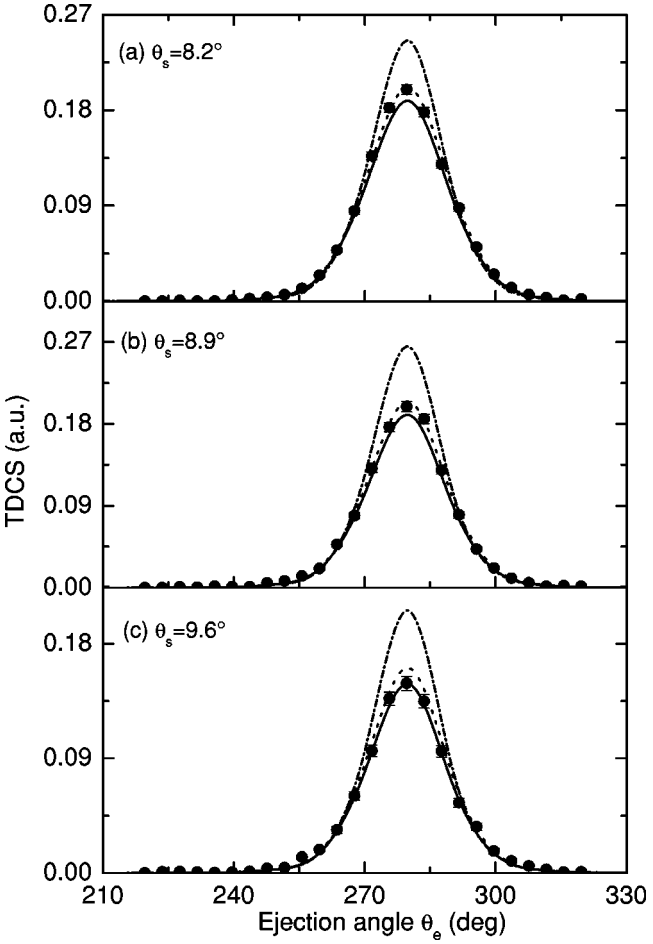

FIG. 3. Same as Fig. 2, but impact energy $E_i=4168$ eV, emission energy $E_e=100$ eV; and scattering angles (a) $\theta_s=8.2°$, (b) $\theta_s=8.9°$, and (c) $\theta_s=9.6°$.

sition of the binary peak is well described by MBBK. The recoil peak region is also well represented at $\theta_s=1°,1.5°$, within experimental error (no experimental results are available for $\theta_s=3°$ in this region). TEC TDCS are also shown in the figures. Both theoretical predictions are in excellent agreement except at the greatest scattering angle for which small discrepancies are observed around the binary-peak region. Results corresponding to twice BBK triple differential cross sections for atomic hydrogen targets computed with the molecule ionization energy are also included in the figures. These results remain practically the same if the atomic binding energy of H is used. This is in accordance with the fact that at this very high impact energy, the bound electron may be considered as almost free. It can be seen that at the smaller scattering angles, i.e., $\theta_s=1°,1.5°$, the atomic BBK cross sections underestimate the experiments, giving figures around 25–30 % lower than the measured binary-peak value. This clearly shows the importance of including the molecular character of the target in the model.

In Figs. 3(a)–3(c), TDCS around the Bethe region at impact and emission energies $E_i=4168$ eV and $E_e=100$ eV, respectively, are studied. In particular, the Bethe condition is satisfied at $\theta_s=8.9°$, i.e., the recoil of the target is zero and all the momentum is transferred to the ejected electron. It can be seen that MBBK TDCS have a good agreement with the experimental results from Ref. [8]. However, a small underestimation of the TDCS is observed at the binary-peak position. BBK TDCS for effective H atoms are also included in the figures. In this case, the maximum values of experiments are overestimated by a factor of 20–35 %.

The situation at lower but still high impact energies is studied in Figs. 4–6 where MBBK triple differential cross sections as a function of the ejection angle θ_e at fixed impact energy E_i and emission energy E_e are presented. In all figures, theoretical predictions are compared with experimental TDCS obtained in a relative scale [5]. In order to make the comparison possible, experimental points appearing in Figs. 4–6 were extracted from the smoothed experimental curves presented in Ref. [5] and normalized to MBBK results at the maximum value corresponding to the binary encounter peak. TEC TDCS are also shown in the figures. In general, there is a very good agreement between MBBK TDCS and experimental data. The position of the binary peak is well reproduced by MBBK TDCS, but systematically slightly shifted to greater angular values with respect to experiments. The

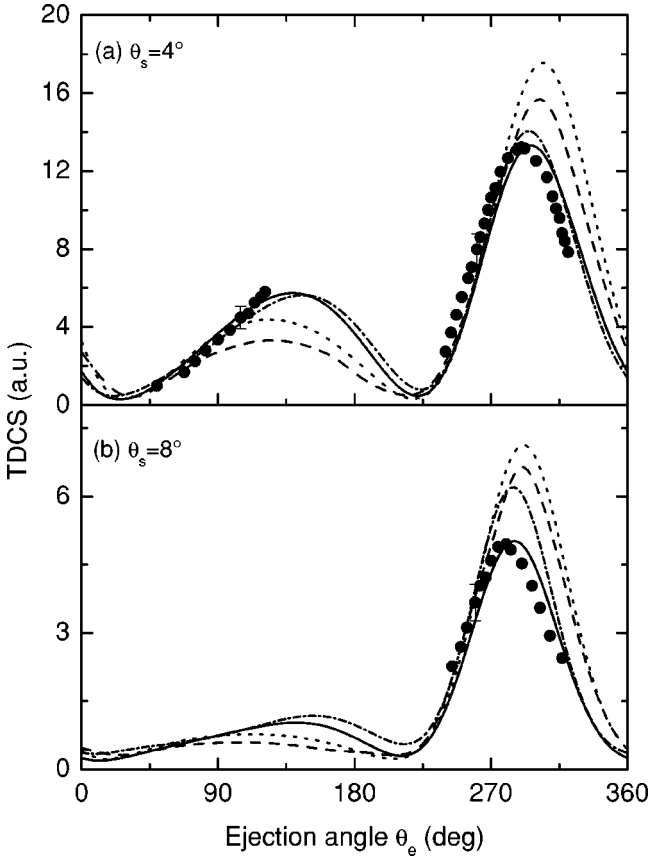

FIG. 4. Same as Fig. 2, but impact energy $E_i = 250$ eV; emission energy $E_e = 4.5$ eV; and scattering angles (a) $\theta_s = 4°$ and (b) $\theta_s = 8°$. Present MBBK results are represented by full lines, TEC results by dotted lines, twice BBK results for effective atomic hydrogen by dashed and dotted lines. DWVA results by dashed lines, and experiments (from Ref. [5]) are represented by full circles.

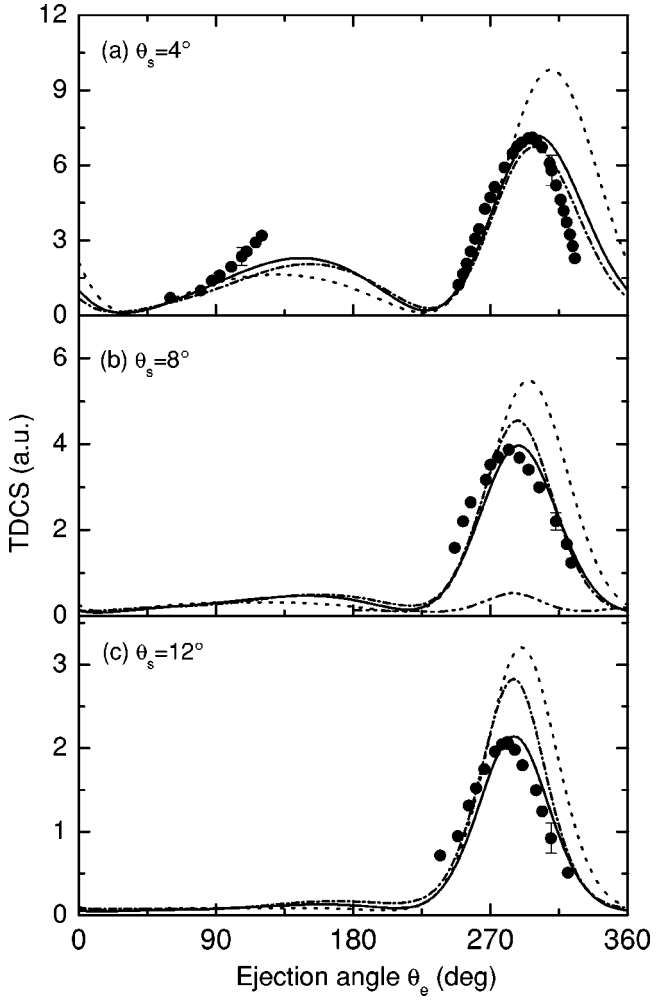

FIG. 5. Same as Fig. 2, but impact energy $E_i = 250$ eV; emission energy $E_e = 9$ eV; and scattering angles (a) $\theta_s = 4°$, (b) $\theta_s = 8°$, and (c) $\theta_s = 12°$. Present MBBK results are represented by full lines, TEC results by dotted lines, twice BBK results for effective atomic hydrogen by dashed and dotted lines. DWBO results by dashed and double dotted lines, and experiments (from Ref. [5]) are represented by full circles.

position of the recoil peak cannot be fully contrasted as only limited measurements are available in this domain. But the general trend of the measurements is well described in this region, except in Fig. 5(a). In this particular arrangement, MBBK results underestimate measurements exhibiting a less pronounced slope, which prevent them from reproducing the sudden rise in measurements. Also in this geometry, MBBK predictions show a broader binary peak, overestimating the experimental data at angles greater than the binary peak. Comparison between TEC and MBBK results leads to the conclusion that TEC values are greater than MBBK at the binary-peak region while the situation is reversed at the recoil peak angular domain. This is similar to the behavior of FBA and BBK for atoms [2], and proves the relevance of including the interaction of the projectile with the ejected electron as the impact energy decreases. The repulsive character of this interaction diminishes the possibility of a binary encounter collision, increasing the electron emission in the backward direction. TEC predictions for the binary-peak position show a marked shift towards greater angles with respect to experiments. This behavior can be also attributed to the repulsive projectile-active electron interaction. Its inclusion in the theoretical description of the reaction provokes a larger relative angular separation between those particles. So, the ejected electron will be reoriented in the binary encounter peak region, to larger angles with respect to the incident direction of the projectile beam. Results obtained as twice the BBK TDCS for effective H atoms with the ionization energy of the molecule are also shown. At $E_i = 250$ eV these estimations are up to 33% greater than the MBBK values around the binary peak. At $E_i = 100$ eV, deviations are also important in the recoil region (see Fig. 6). The departure from the MBBK results increases if the true binding energy of the H atoms is used.

In order to compare with other theories, TDCS obtained with a distorted-wave velocity approximation (DWVA) [12] and with a distorted-wave model within the Born-Oppenheimer approximation (DWBO) [9] are included in Figs. 4 and 5(b), respectively. In DWVA, the transition matrix element is calculated in its velocity form, and the wave functions corresponding to the high-energy incident and scattered electrons are treated as plane waves. The interaction of

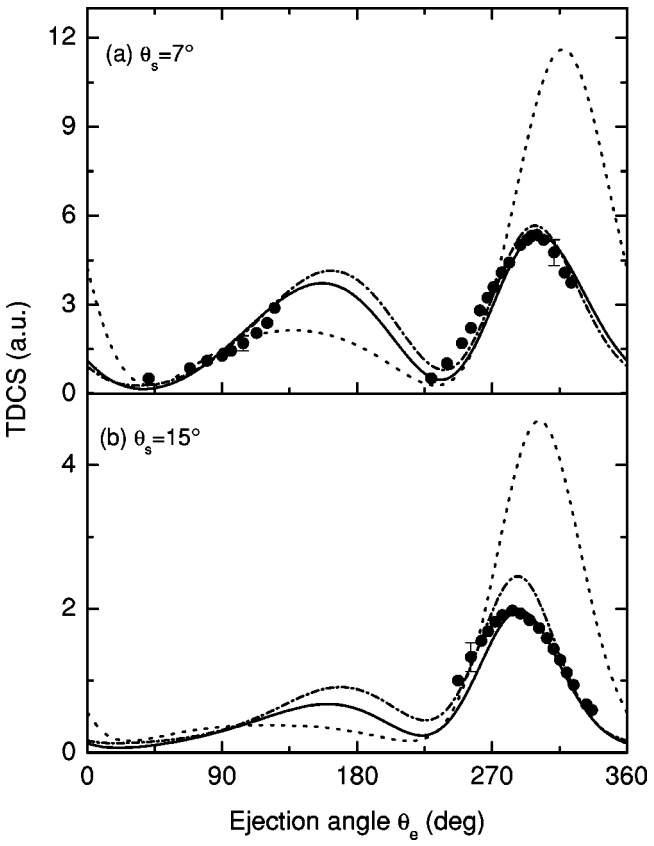

FIG. 6. Same as Fig. 2, but impact energy $E_i = 100$ eV; emission energy $E_e = 4.5$ eV; and scattering angles (a) $\theta_s = 7°$ and (b) $\theta_s = 15°$.

the ejected electron with the ionized target is approximated by means of the static-exchange potential evaluated in the frozen-core Hartree-Fock approximation. In DWBO, the wave function of the incoming electron is calculated in the static-exchange potential field generated by a neutral H_2 molecule, whereas those of the two outgoing electrons are calculated in the static-exchange potential field of the H_2^+ ion. In contrast, the projectile-active electron interaction is considered only in a first-order approximation in both models. DWVA results shown in Fig. 4 do not present relevant differences with respect to the TEC model. Surprisingly, the DWBO TDCS underestimate the ones obtained with the MBBK model by almost one order of magnitude. The double-differential cross sections (DDCS) as a function of the scattering angle obtained in this DWBO approximation present a good qualitative agreement with available experiments [9]. However, at incident energy $E_i = 250$ eV and emission energies $E_e = 100$, 117.3 eV, the DDCS underestimate absolute DDCS data at large and small scattering angles. Unfortunately, DDCS for $E_e = 9$ eV analyzed in Fig. 5(b) were not reported in Ref. [9]. As stated by the authors in Ref. [9], their distorted-wave model neglects multichannel effects as well as postcollisional correlation between the two outgoing electrons. On the contrary, these effects are taken into account in the MBBK approach and may be the reason of the observed differences.

IV. CONCLUSIONS

A molecular BBK model has been developed within the framework of a two-effective-center approximation to study ionization of H_2 molecules. In this model, the molecular structure of the target as well as the correlated motion of the particles in the final channel of the reaction are taken into account. The latter fact is accomplished by means of a three-continuum function. The agreement of calculated TDCS with available experiments is satisfactory. The present approach may be useful in studying other simple diatomic molecules such as N_2, where the electron distributions are less concentrated at nuclei than in the H_2 case. For instance, the involved molecular orbitals can be modelized by means of a linear combination of atomic orbitals in a self-consistent field [23], as it was previously made in the framework of heavy-ion impact [24]. Finally, it is worthy to mention that the MBBK computational scheme is, in general, more time consuming than the TEC one. However, MBBK results are easily obtained with a standard PC working on Linux.

ACKNOWLEDGMENT

This work was partially supported by the French-Argentinean ECOS-Sud program (Grant No. A98E06). C.R.S., O.A.F., and R.D.R. also acknowledge support from the Agencia Nacional de Promoción Científica y Tecnológica (BID 802/OC-AR PICT; Grant No. 03-04262) and the Consejo Nacional de Investigaciones Científicas y Técnicas de la República Argentina.

[1] M. E. Rudd and R. D. DuBois, Phys. Rev. A **16**, 26 (1977).
[2] M. Brauner, J. S. Briggs, and H. Klar, J. Phys. B **22**, 2265 (1989).
[3] G. Garibotti and J. E. Miraglia, Phys. Rev. A **21**, 572 (1980).
[4] H. Ehrhardt, G. Knoth, P. Schlemmer, and K. Jung, Phys. Lett. **110A**, 92 (1985).
[5] K. Jung, E. Schubert, D. A. L. Paul, and H. Ehrhardt, J. Phys. B **8**, 1330 (1975).
[6] R. D. DuBois and M. E. Rudd, Phys. Rev. A **17**, 843 (1978).
[7] T. W. Shyn, W. E. Sharp, and Y.-K. Kim, Phys. Rev. A **24**, 79 (1981).
[8] M. Chérid, A. Lahmam-Bennani, R. W. Zurales, R. R. Lucchese, A. Duguet, M. C. Dal Capello, and C. Dal Capello, J. Phys. B **22**, 3483 (1989).
[9] A. L. Monzani, L. E. Machado, M.-T. Lee, and A. M. Machado, Phys. Rev. A **60**, R21 (1999).
[10] I. E. McCarthy, J. Phys. B **6**, 2358 (1973).
[11] S. Dey, I. E. McCarthy, P. J. O. Teubner, and E. Weigold, Phys. Rev. Lett. **34**, 782 (1975).
[12] R. W. Zurales and R. R. Lucchese, Phys. Rev. A **37**, 1176 (1988).
[13] F. Elboudali and B. Joulakian, J. Phys. B **34**, 4877 (2001).

[14] P. Weck, O. A. Fojón, B. Joulakian, C. R. Stia, J. Hanssen, and R. D. Rivarola, Phys. Rev. A **66**, 012711 (2002).
[15] P. Weck, O. A. Fojón, J. Hanssen, B. Joulakian, and R. D. Rivarola, Phys. Rev. A **63**, 042709 (2001).
[16] J. Berakdar, Phys. Rev. Lett. **81**, 1393 (1998).
[17] A. Köver and G. Laricchia, Phys. Rev. Lett. **80**, 5309 (1998).
[18] S. C. Wang, Phys. Rev. **39**, 579 (1928).
[19] O. A. Fojón, R. D. Rivarola, J. Hanssen, and M. Ourdane, Phys. Rev. A **55**, 4613 (1997), and references therein.
[20] C. A. Coulson, Proc. Cambridge Philos. Soc. **38**, 210 (1942).
[21] C. R. Stia, O. A. Fojón, and R. D. Rivarola, J. Phys. B **33**, 1211 (2000).
[22] O. A. Fojón, R. D. Rivarola, R. Gayet, J. Hanssen, and P. A. Hervieux, J. Phys. B **30**, 2199 (1997).
[23] C. W. Scherr, J. Chem. Phys. **23**, 569 (1955).
[24] M. E. Galassi, R. D. Rivarola, M. Beuve, G. H. Olivera, and P. D. Fainstein, Phys. Rev. A **62**, 022701 (2000).